ISBN: 978-3-95450-245-5 ISSN: 2226-0374 doi:10.18429/JACoW-COOL2023-THPAM1R3

STATUS OF E-COOLING CHARACTERISATION AT 100 keV IN ELENA

D. Gamba*, F. Asvesta, P. Kruyt[1], L. Ponce, and G. Russo
CERN, 1211 Geneva, Switzerland
[1] also at Goethe University, Frankfurt, Germany

Abstract

The Extra Low ENergy Antiproton ring (ELENA) ring at CERN was commissioned in 2018 and has been in regular production operation since 2021. ELENA uses e-cooling for cooling antiproton (pbar) beams on two plateaus at 653 keV and 100 keV kinetic energy. The first cooling is necessary to allow for efficient deceleration of the 5.3 MeV pbar beam coming from the Antiproton Decelerator (AD), while the second cooling is used to define the quality of the bunches before extraction. The experience accumulated so far shows that cooling at 653 keV is sufficient to ensure good deceleration efficiency, while cooling at 100 keV might not be enough to provide the design transverse beam emittances at extraction. In this paper, we document the present ELENA e-cooling performance at 100 keV, the typical optimisation procedure used during setup, and we investigate possible limitations of the present system.

INTRODUCTION

The ELENA ring is part of the Antimatter Factory at CERN, which is a unique facility that provides pbar beams for low energy antimatter physics [1, 2]. Pbars are produced in the AD target area by sending a 26.4 GeV/c proton beam on an iridium-based target. The emerging pbars at 3.575 GeV/c are guided and collected into the AD ring which cools and decelerates them down to 5.3 MeV kinetic energy. They are then transferred to the ELENA ring which further decelerates and cools them down to 100 keV kinetic energy. Here, four bunches are produced and distributed to up to four experiments at the same time. An overall parameter to assess the antimatter factory performance is the number of pbars delivered to the users as a function of protons sent on target. This is shown in Fig. 1, in which about four weeks of data from 2022 is compared to an equivalent period in 2023. Continuous optimisation of the AD target area and transport allows to regularly reach a pbar yield of 3×10^{-6} pbar injected in AD per proton delivered on target. Proton intensity from the CERN injectors was increased during 2022 and 2023 runs in steps from about 1.4×10^{13} to about 1.7×10^{13}. This, together with improved deceleration efficiency, allowed to increase the number of pbars to more than 5×10^{7} injected in AD and more than 4×10^{7} in ELENA. Each user requesting beam is now typically receiving 9×10^{6} pbar, which is about a factor of 2 higher than the design value.

In the following sections, an update on the ELENA cycle and its hardware will be outlined followed by the latest measurements of e-cooling characterisation with emphasis on the extraction plateau at 100 keV.

* davide.gamba@cern.ch

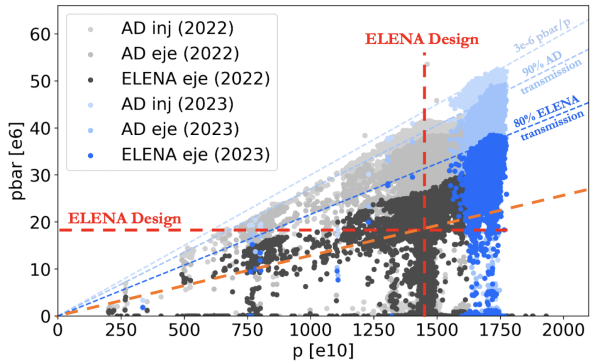

Figure 1: Antiproton intensity as a function of protons on AD target. Pbars measured at AD injection, ELENA injection and ELENA extraction are indicated from lighter to darker colors. Shades of black and blue indicate 2022 and 2023 data, respectively. Proton on target and ELENA extraction design parameters are also indicated in dashed red.

ELENA CYCLE AND INSTRUMENTATION

The ELENA magnetic cycle and available instrumentation are basically unchanged with respect to what is reported in [3]. On top of the regular operation with pbar, ELENA can still be operated with H^- from its local source [4, 5], which continues to be an essential asset for machine setup.

The typical magnetic cycle, basically identical for both pbar and H^- operation, is shown in Fig. 2. During H^- operation the beam is injected at the lowest plateau at 100 keV, it is accelerated to pbar injection energy (5.3 MeV), and then it follows the nominal deceleration cycle as for the pbar. The lifetime of H^- beam is of the order of 5 s, mainly driven by the average ring pressure level which settled at about 1×10^{-11} mbar, while no sizable lifetime degradation via interaction with the electron beam of the e-cooler has been observed so far.

Due to the sizeable H^- beam intensity reduction after deceleration, a second injection at the beginning of the last e-cooling plateau is performed, so to obtain H^- beams at extraction of comparable intensities to the pbar ones.

The ELENA e-cooler [6] was commissioned in 2018 [7], and so far did not require any modifications nor major maintenance. Its main parameters are summarised in Table 1. Since e-cooler parameters cannot be quickly changed between H^- and pbar cycles operation, and hence the electron velocity is fixed, the H^- momentum at the different plateaus is adjusted to match the pbar revolution frequency.

The main instrumentation for e-cooling setup and adjustment remains the Schottky signal, which in ELENA is obtained by combining the signal of several Beam Position

ISBN: 978-3-95450-245-5 ISSN: 2226-0374 doi:10.18429/JACoW-COOL2023-THPAM1R3

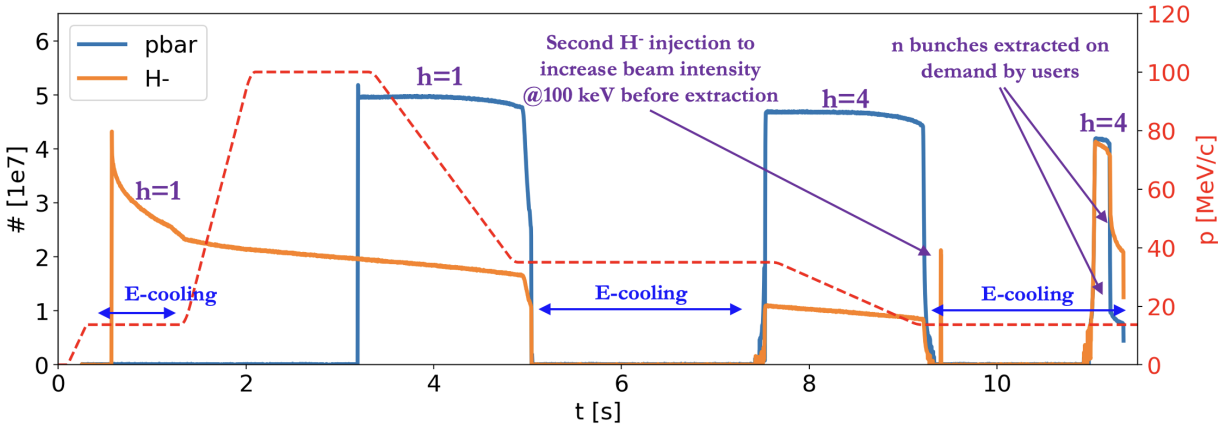

Figure 2: H^- (orange) and pbar (blue) beam intensity along a typical ELENA cycle (dashed red). Intensity signal is visible only when the beam is bunched. Key points and observations are highlighted.

Monitor (BPM) pickups [8]. A typical spectrogram obtained by this system along the 100 keV plateau with H^- is shown in Fig. 3. To be noted the second H^- injection at about 9.4 s from the start of the cycle, which is longitudinally cooled in a few hundred ms, and the start of the RF at about 11.8 s, where synchrotron side-bands show up.

The main instrument for transverse beam profile measurements in the ELENA ring is based on a scraper blade [9, 10], which measures the secondary emission from losses induced by the moving blade progressively approaching the beam closed orbit. Characterisation of this instrument is ongoing [11], however, it remains of limited use due to the observed fast cooling time with respect to the typical measurement time of a few hundred ms. Moreover, if for pbar one can obtain clean loss signals, the measurement of H- based on in-vacuum microchannel plates (MCPs) is more sensitive to noise and difficult to interpret.

A monitor to measure neutral hydrogen atoms escaping the ELENA ring is installed on the e-cooler straight section. Its interpretation is also being studied [12], but this system is not yet used for e-cooling setup and operation.

Transverse e-cooling characterisation at 100 keV is typically done by profiting of the semi-intercepting micro-

Table 1: ELENA E-Cooler Main Parameters

Parameter	ELENA	
Pbar p [MeV/c]	35	13.7
Pbar E_k [MeV]	0.635	0.1
e^- E_k [keV]	0.355	0.055
β_{rel}	0.037	0.015
I_{e^-} [mA]	5	1
Cooler L [m]	1	
Ring L [m]	30.41	
Gun B [G]	up to 1000	
Drift B [G]	100	
Drift $B_\perp/B_\parallel$	$< 5 \times 10^{-3}$	
e^- beam r [mm]	8 to 25	

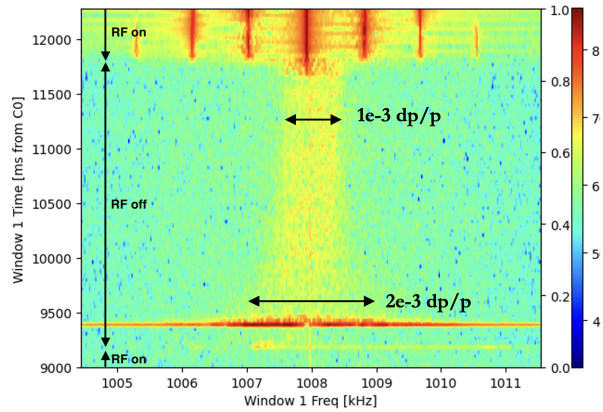

Figure 3: Spectrogram of the Schottky signal measured along the 100 keV extraction plateau in ELENA with H^- beams.

wire monitors, also called Secondary Emission Monitors (SEMs) [13], installed in the ELENA-extraction transfer lines. Using several of those monitors inserted into the beam path allows to perform a multi-profile Twiss measurement, as shown for example in Fig. 4. This method is regularly used to monitor extracted beam performance. Approximately 10% of beam intensity is lost during the passage in each SEM monitor inserted into the beam. Therefore, several monitors can be inserted in the beam line only during dedicated machine development times, while typically a single monitor is used to log the beam profile stability or for parasitic machine development with H^-.

Effort is being put into producing a simulation framework [14] based on the Parkhomchuk model [15] of e-cooling to allow for modelling the expected cooling performance for different machine configurations. For example, Fig. 5 shows a preliminary study to estimate of the impact of the e-cooler magnetic field imperfection on the cooling time in ELENA at 100 keV neglecting heating effects. To be noted that the ELENA e-cooler magnetic field imperfection is somewhere below 5×10^{-3} (Table 1), hence some degra-

ISBN: 978-3-95450-245-5 ISSN: 2226-0374 doi:10.18429/JACoW-COOL2023-THPAM1R3

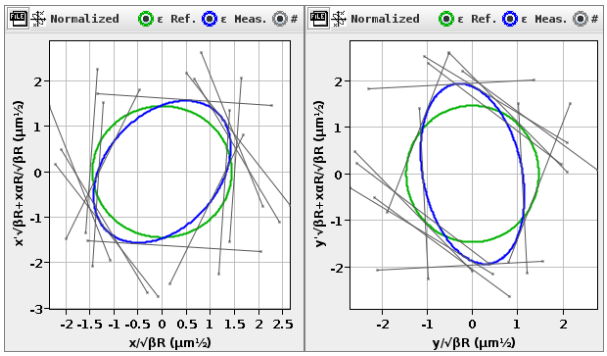

Figure 4: Horizontal (left) and vertical (right) transverse Twiss measurement (blue) compared to the nominal TWISS ellipse (green) in normalised phase space. Gray lines correspond to beam sizes measured by several SEM's along the LNE00 transfer line.

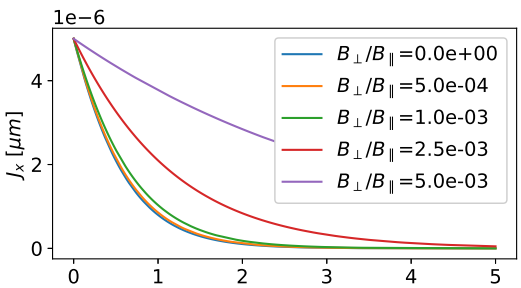

Figure 5: Simulated time evolution of horizontal action of a single particle representing the beam envelope for different e-cooler magnetic field quality: perfect magnetic field (blue), $B_\perp/B_\parallel = 5 \times 10^{-4}$ (orange), 1×10^{-3} (green), 2.5×10^{-3} (red), and 5×10^{-3} (purple).

dation of the cooling time with respect to an ideal magnetic field is to be expected. The cooling time should be of the order of a second, which is indeed compatible with what observed so far.

EXTRACTED BEAM CHARACTERISATION

The beam is re-bunched before extraction at harmonic four while e-cooling is kept on, hence bunched-beam cooling is performed for reaching minimum energy spread and bunch length. The intensity of the extracted bunches is much above the design value of 4.5×10^6 , see Fig. 1. With the present machine working point, it was observed that e-cooler currents above 1 mA result in beam losses when the bunch length reaches a minimum of about 150 ns Full Width Half Maximum (FWHM). Hence, the e-cooler is typically set to deliver about 0.5 mA on the 100 keV plateau, such to ensure that no or minimum beam losses are produced during bunched-beam cooling. The obtained bunch length is close to the ELENA design value [16], but some users prefer to have even shorter bunches and 100 ns-long FWHM bunches are obtained by performing bunch rotation just before extraction. The corresponding bunch rms momentum spread is less than 1×10^{-3}, while, for bunches without bunch rotation, it is less than 5×10^{-4}.

The transverse cooling setup and optimisation are mainly done by monitoring the size of the extracted beam. This can be performed without re-bunching the beam before extraction in order to decouple the coasting beam e-cooling performance from effects linked to the re-bunching and/or from the bunched-beam cooling before extraction. In this case, all the beam is extracted towards a transfer line. The horizontal sweep of the particles extracted during the rise time of the extraction kicker (less than 1 μs) does not seem to be sizeable compared to the total particle stream length of 7 μs, which corresponds to the ring revolution period.

Figure 6 shows an example optimisation of the angle between e^- trajectory and, in this case, H^- orbit inside the e-cooler: while the e^- beam trajectory is not changed, the H^- beam closed-orbit angle inside the e-cooler is varied over consecutive cycles using four correctors in the e-cooler straight section. The beam size in the ELENA extraction is measured on a SEM grid after each cycle, and the H^- orbit that minimises the beam size is chosen as optimum.

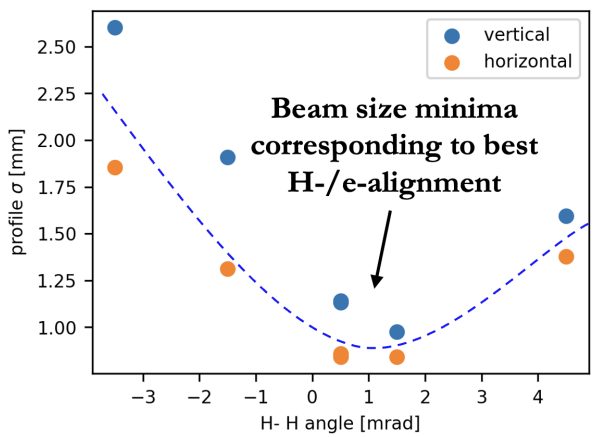

Figure 6: Horizontal (orange) and Vertical (blue) beam size measured on a SEM grid in the ELENA extraction line as a function of the H^- closed orbit angle in the e-cooler. The dashed blue line only serves to guide the eyes.

In a similar way, the minimum length of the e-cooling plateau can be found by varying cycle-to-cycle beam extraction time, as shown in Fig. 7. In this measurement, one can see that the extracted beam size flattens out after about 1.5 s from the second H^- beam injection, which is performed at $t = 9.4$ s into the cycle (See Fig. 2).

Our future plan is to perform these kind of measurements in a more systematic way and to compare the obtained results between H^- and pbars, as well as with simulations. To be noted that these methods do not allow to evaluate the cooling performance of the tails of the transverse beam distribution, because they are not easily detectable by the SEM profile monitor. This kind of analysis will need to be done using

ISBN: 978-3-95450-245-5 ISSN: 2226-0374 doi:10.18429/JACoW-COOL2023-THPAM1R3

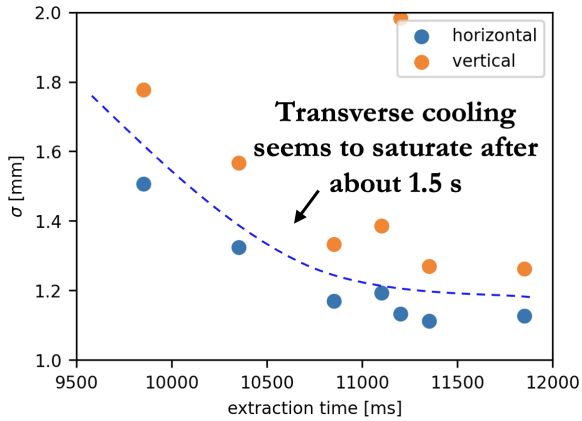

Figure 7: Horizontal (orange) and Vertical (blue) beam size measured on a SEM grid in the ELENA extraction line as a function of extraction beam time. The dashed blue line only serves to guide the eyes.

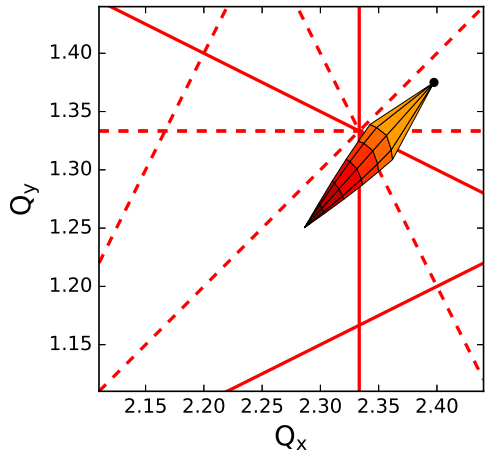

Figure 8: Tune footprint due to space charge for a typical bunch at ELENA extraction energy for the present working point ($Q_x = 2.3975$, $Q_y = 1.375$). Normal (solid) and skew (dashed) resonance up to the third order are also shown.

scrapers inside the ring, which is also the subject of future studies.

RECENT DEVELOPMENT

Despite having good control of the e-cooler setup, the measured transverse emittances of the extracted bunched beams are about a factor of two higher than the design values. Most users do not seem to be strongly affected by the larger beam size, but investigations are ongoing to see if this limitation could be overcome.

Previous observations have already shown that the extracted beam emittance is dependent on the beam intensity [3]. This observation, together with the beam losses observed when reaching even shorter bunches with aggressive bunched-beam cooling, suggests a space-charge-driven effect.

The tune spread due to direct space charge for a Gaussian beam can be computed using the approach described in [17]. Assuming a bunch of 1×10^7 pbars, 150 ns FWHM bunch length, 2 µm rms geometric transverse emittances and the nominal ELENA optics [18], one obtains the tune footprint shown in Fig. 8, which correspond to a maximum tune spread of about 0.1. To be noted that the tune footprint for the bunched beam crosses several third-order resonances. For a coasting beam, and assuming 4×10^7 pbars, the tune spread drops to about 0.01, and no resonances are crossed. The present working hypothesis is that the beam interacts with a not-corrected third-order resonance during and after the bunching process takes place, and this leads to emittance growth and eventually beam losses.

Tune scans have been performed to investigate this hypothesis. Figure 9 shows an example of such a measurement. The beam, after cooling, is re-bunched as usual and kept in the machine for about 1 s. This is presently the only way to have a measurement of beam intensity inside the ring. In order to subtract the natural loss of H^- due to vacuum interaction, an exponential compensation of the measured beam intensity is applied assuming a lifetime of 5.5 s. While the beam is bunched, the machine working point is moved linearly over time, and the loss rate as a function of the working point is logged. By performing such a measurement starting also from different vertical working points, one obtains the map shown in Fig. 10. This preliminary measurement suggests that a strong third-order resonance ($Q_x = 2.33$) is indeed present, and it cannot be approached without encountering considerable beam losses. Other beam-loss mechanisms at higher horizontal tunes seem to be also present. So far no scans of the working point at a lower vertical tune have been performed. More detailed measurements are envisaged to extend the explored parameter space and to better understand the observed beam losses.

From the tune diagram in Fig. 8 one might desire to move the working point below the third-order resonances. A first attempt to do so before re-bunching was unsuccessful (all

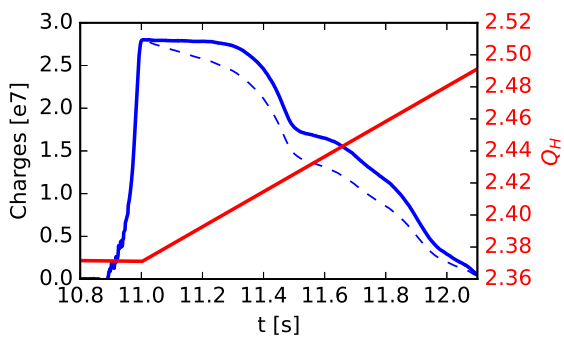

Figure 9: Raw (dashed blue) and lifetime-compensated (solid blue) intensity measurement of an H^- beam during and after recapture at 100 keV. At the end of the recapture process ($t = 11$ s), the set horizontal tune (red) is varied linearly.

ISBN: 978-3-95450-245-5 ISSN: 2226-0374 doi:10.18429/JACoW-COOL2023-THPAM1R3

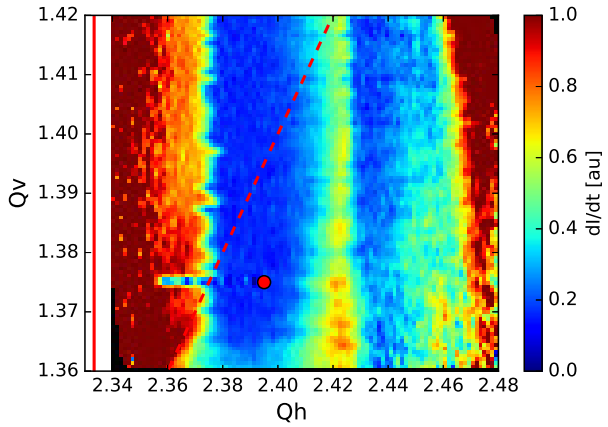

Figure 10: Beam intensity loss rate as a function of working point measured with several horizontal tune scan measurements with H^- beam. The nominal working point used as the start for all measurements is shown as a red dot. The horizontal third-order resonance (solid red) and the second-order coupling resonance (dashed red) are also shown.

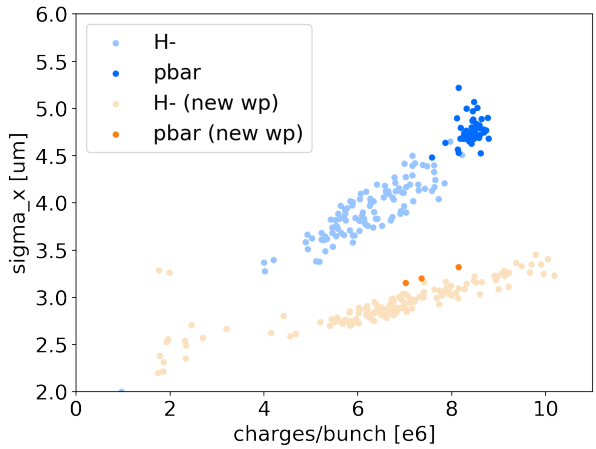

Figure 11: Measured horizontal beam size as a function of bunch intensity measured on a single SEM in the ELENA extraction line for the old (blue) and new (orange) machine working point using H^- (light) and pbars (dark).

beam was lost), hence an attempt was made by modifying the working point of the whole ELENA cycle. Empirically, it was found that by setting the tunes at about $Q_x = 2.30$ and $Q_y = 1.32$ the machine could be operated without major losses along the whole cycle both for H^- and pbar beams. Figure 11 shows a comparison of the beam size measured in the ELENA transfer line over consecutive cycles with the previous and new working points. Note that pbar cycle intensities are typically more stable than the H^- ones, as the latter suffers from a known shot-to-shot intensity instability of the ELENA H^- source. This is useful to naturally show the dependency of extracted beam size/emittance on intensity. It was only possible to collect data from three pbar cycles with the new working point, as this measurement was done during physics time and not in a dedicated machine development slot. Nevertheless, it is interesting to observe

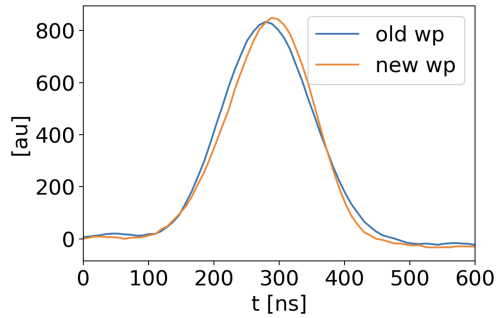

Figure 12: Longitudinal pbar bunch profile measured by a longitudinal profile monitor in ELENA extraction line for the old (blue) and new (orange) working point for two pbar cycles with intensities of about 8×10^6 pbars/bunch.

how the pbar cycles overlap well with the trend shown by the H^- cycles, demonstrating the good equivalence between the two particles/cycles. The significantly reduced beam size is evident. The bunch length obtained with the two working points is comparable, as shown in Fig. 12, hence the difference in transverse beam size cannot be due to reduced line density of the bunch.

The difference in beam size could also be explained by beta beating due to the change of working point, but independent measurements using several SEM monitors, not shown here, suggest that emittances have indeed been reduced by about a factor of two. Additional investigations are necessary to confirm this preliminary result, and possibly further improve the working point and hence the emittances of the beams delivered to the users.

CONCLUSION

The Antimatter Factory at CERN and especially the ELENA ring have demonstrated to reliably achieve the design beam performance, except for transverse beam emittance. The availability of H^- beam is fundamental for machine setup and in particular for e-cooling studies. No degradation of the H^- beam lifetime with e-cooling has been observed and the cooling performance seems to be equivalent between pbar and H^- beams.

Work is continuously ongoing to better characterise the beam instrumentation and hence better control the beam and further improve the beam quality. For example, the preliminary studies presented in this paper pave the way towards the possibility of achieving the design transverse beam emittances despite the much higher beam intensity compared to the design.

Effort is also being put into developing e-cooling simulation tools that will hopefully allow for the exploration of fundamental e-cooling physics processes, for example, the impact of transverse field quality on the cooling time.

ACKNOWLEDGEMENTS

The authors acknowledge the CERN Beam Instrumentation colleagues in charge of the CERN e-coolers and the

ISBN: 978-3-95450-245-5 ISSN: 2226-0374 doi:10.18429/JACoW-COOL2023-THPAM1R3

AD/ELENA operation crew for their invaluable support and dedication.

REFERENCES

[1] M. Hori and J. Walz, "Physics at CERN's Antiproton Decelerator", *Prog. Part. Nucl. Phys.*, vol. 72, pp. 206–253, Sep. 2013. doi:10.1016/j.ppnp.2013.02.004

[2] C. Carli *et al.*, "ELENA: Bright Perspectives for Low Energy Antiproton Physics", *Nucl. Phys. News*, vol. 32, no. 3, pp. 21–27, 2022. doi:10.1080/10619127.2022.2100646

[3] D. Gamba, L. Bojtár, C. Carli, B. Dupuy, A. Frassier, L.V. Jørgensen, *et al.*, "AD/ELENA Electron Cooling Experience During and after CERNs Long Shutdown (LS2)", in *Proc. COOL'21*, Novosibirsk, Russia, Nov. 2021, pp. 36–41. doi:10.18429/JACoW-COOL2021-S503

[4] A. Megía-Macías, R. Gebel and B. Lefort, "The ion source for the commissioning of ELENA ring", in *Proc. ICIS'2017*, Geneva , Switzerland, Oct. 2017, vol. 2011, no. 1, p. 090014. doi:10.1063/1.5053395

[5] D. Gamba *et al.*, "Operational experience with the ELENA ion source", in *AIP Conf. Proc. NIBS 2020*, Online, Sep. 2020, vol. 2373, no. 1, p. 040005. doi:10.1063/5.0057535

[6] G. Tranquille *et al.*, "The ELENA Electron Cooler", in *Proc. IPAC'16*, Busan, Korea, May 2016, pp. 1236–1238. doi:10.18429/JACoW-IPAC2016-TUPMR006

[7] G. Tranquille, J. Cenede, S. Deschamps, A. Frassier, and L.V. Jørgensen, "Commissioning the ELENA Electron Cooler", presented at COOL'19, Novosibirsk, Russia, Sep. 2019, paper TUPS12, unpublished.

[8] O. Marqversen and S. Jensen, "Schottky Signal From Distributed Orbit Pick-Ups", in *Proc. IBIC'21*, Pohang, Korea, Sep. 2021, pp. 366–369. doi:10.18429/JACoW-IBIC2021-WEPP04

[9] P. Grandemange, "Preliminary simulation with Geant4 for the AD scraper renovation", CERN, Geneva, Switzerland, Oct. 2016.

[10] J. R. Hunt, "Beam Quality Characterisation and the Optimisation of Next Generation Antimatter Facilities", Ph.D. Thesis, U. Liverpool, United Kingdom, 2019.

[11] G. Russo, B. Dupuy, D. Gamba and L. Ponce, "Transverse emittance reconstruction along the cycle of the CERN Antiproton Decelerator", presented at HB'23, Geneva, Switzerland, Oct. 2023, paper THC1C1, unpublished.

[12] G. Tranquille *et al.*, "H0 Diagnostics for the ELENA Electron Cooler", presented at COOL'23, Montreux, Switzerland, Oct. 2023, paper THPOSRP09, this conference.

[13] M. Hori, "Photocathode Microwire Monitor for Nondestructive and Highly Sensitive Spatial Profile Measurements of Ultraviolet, X-Ray, and Charged Particle Beams", *Rev. Sci. Instrum.*, vol. 76, no. 11, p. 113303, 2005. doi:10.1063/1.2130931

[14] P. Kruyt, G. Franchetti, and D. Gamba, "Advancements and Applications of Cooling Simulation Tools: A Focus on Xsuite", presented at COOL'23, Montreux, Switzerland, Oct. 2023, paper THPOSRP02, this conference.

[15] V. V. Parkhomchuk, "New insights in the theory of electron cooling", *Nucl. Instr. Meth.*, vol. 441, no. 1, pp. 9–17, 2000. doi:10.1016/S0168-9002(99)01100-6

[16] V. Chohan (ed.) *et al.*, "Extra Low ENergy Antiproton (ELENA) ring and its Transfer Lines: Design Report", CERN, Geneva, Switzerland, Rep. CERN-2014-002, Jan. 2014.

[17] F. Asvesta and H. Bartosik, "Resonance Driving Terms From Space Charge Potential", CERN, Geneva, Switzerland, Rep. CERN-ACC-NOTE-2019-0046, Oct 2019.

[18] D. Gamba *et al.*, "ELENA Commissioning", in *Proc. NA-PAC'19*, Lansing, MI, USA, Sep. 2019, pp. 626–631. doi:10.18429/JACoW-NAPAC2019-WEYBB1